

Analysis of Thermal and Mechanical Parameters of the BFRP Bars [†]

Małgorzata Wydra ^{1,*}, Piotr Dolny ¹, Grzegorz Sadowski ¹, Natalia Grochowska ², Piotr Turkowski ³
and Jadwiga Fangrat ³

¹ Faculty of Civil Engineering, Mechanics and Petrochemistry, Warsaw University of Technology, Lukasiewiczza 17, 09-407 Płock, Poland

² Faculty of Physics, Warsaw University of Technology, Koszykowa 75, 00-662 Warsaw, Poland

³ Building Research Institute, Filtrowa 1, 00-611 Warsaw, Poland

* Correspondence: malgorzata.wydra@pw.edu.pl; Tel.: +48-505-225-741

[†] Presented at the 10th MATBUD'2023 Scientific-Technical Conference "Building Materials Engineering and Innovative Sustainable Materials", Cracow, Poland, 19–21 April 2023.

Abstract: Fibre-Reinforced Polymer (FRP) reinforcement bars are gaining interest in terms of using them as an internal reinforcement in concrete construction parts due to their high tensile strength, corrosion resistance, low weight, and electrical indifference. Nevertheless, low elasticity and difficulties related to a high reduction in mechanical properties at even slightly elevated temperatures seem to limit this potential, due to existing fire safety requirements for buildings. Basalt FRP, which is the subject of this experimental study, is a relatively new type of non-metallic bars, and their environmental friendliness has been underlined in previous studies. The aim of this study is to determine the mechanical properties of BFRP bars, such as tensile and compressive strength and elasticity modulus, at normal and elevated temperatures up to 200 °C. The medium values of compressive strength at room temperature were in the range of 441.2–466.8 MPa, and it was significantly lower than the tensile strength (930.5–1121.3 MPa). Additionally, low values of elasticity modulus, especially when comparing to steel bars (typically about 210 GPa), were found in both compression (mean values: 31.0–38.4 GPa) and tension (mean values: 43.3–44.6 GPa). Low elasticity modulus may lead to difficulties with excessive deflections and crack widths, when designing bent elements with such reinforcement. Moreover, reduced mechanical properties at compression should not be neglected when designing compressed parts. Additionally, the phase change parameters, e.g., glass transition temperature, have been determined by means of DMA method, and the glass transition temperature was found to be equal to 107.5 °C.

Keywords: Basalt Fibre-Reinforced Polymer; reinforcement; temperature



Citation: Wydra, M.; Dolny, P.; Sadowski, G.; Grochowska, N.; Turkowski, P.; Fangrat, J. Analysis of Thermal and Mechanical Parameters of the BFRP Bars. *Mater. Proc.* **2023**, *13*, 24. <https://doi.org/10.3390/materproc2023013024>

Academic Editors: Katarzyna Mróz, Tomasz Tracz, Tomasz Zdeb and Izabela Hager

Published: 15 February 2023



Copyright: © 2023 by the authors. Licensee MDPI, Basel, Switzerland. This article is an open access article distributed under the terms and conditions of the Creative Commons Attribution (CC BY) license (<https://creativecommons.org/licenses/by/4.0/>).

1. Introduction

Fibre-Reinforced Polymer (FRP) is a light, high-strength, and durable material. Its electric indifference, high corrosion resistance, high tensile strength, good damage tolerance, good fatigue performance and low energy consumption during the fabrication of raw materials should also be highlighted [1–8]. These advantages make them potentially attractive as an alternative to traditional reinforcement. Nevertheless, there are also important disadvantages, when comparing FRP to steel, which may significantly influence the performance of such a reinforcement in concrete building structures. One of these disadvantages is the fact that FRPs have much lower compressive strength than the tensile strength, another that they have a low elasticity modulus and, finally, poor mechanical performance at even slightly elevated temperatures.

This study aims to analyse thermal and mechanical properties of the basalt type of FRP, which is relatively new and has not as yet been sufficiently examined [9]. The environmental

impact of BFRP composites (especially in terms of costs and amount of energy during production) should be emphasised, as it is lower when compared to CFRP [10].

2. Materials and Specimens

Three diameters of the same type of BFRP bars were tested: 8, 10, and 12 mm. The fibre content was equal to 77%, and epoxy type of matrix was used. Precise diameters of the bars were measured in five random locations along the bars and were equal to 8.1 ± 0.2 , 9.2 ± 0.1 and 11.6 ± 0.3 (mean value \pm standard deviation), respectively.

A cuboid specimen was cut out of the inner part of the $\text{Ø}12$ BFRP bar, with the cross section of 9.64 mm and 3.28 mm, on which Dynamic Mechanical Analysis was performed in order to determine the glass transition temperature of the analysed BFRP material.

$\text{Ø}10$ and $\text{Ø}12$ BFRP bars with the length of 1 m were tested in tension. In that case, 330 mm-long steel pipes were mounted at the end specimens in order to prevent crushing of the FRP in the grip of the hydraulic press (see Figure 1). Either epoxy resin (for $\text{Ø}10$ BFRP specimens) or expansive mortar ($\text{Ø}10$ and $\text{Ø}12$) was used to attach the FRP bars into the steel pipes.



Figure 1. Specimens for tension tests ($\text{Ø}12$ BFRP, steel caps mounted with the use of expansive mortar).

The specimens in compression at both room and elevated temperatures were tested with the use of steel caps (see Figure 2a), similarly to experiments performed by Khorramian and Sadeghian [11].

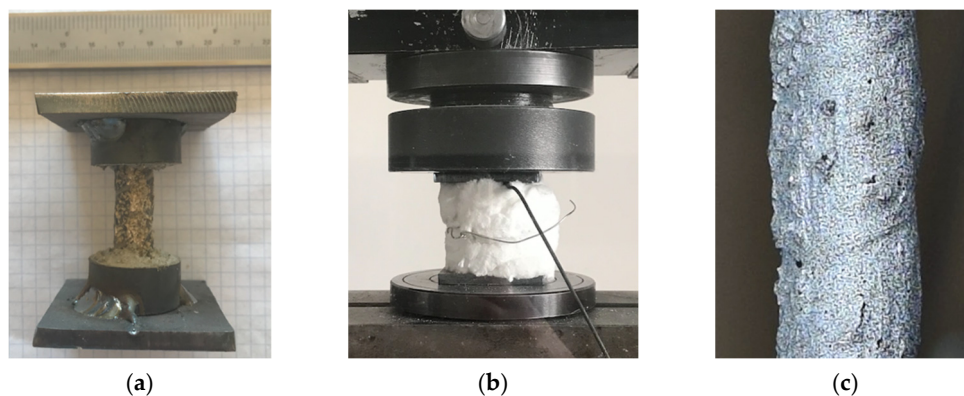


Figure 2. Specimen for compressive strength test ($\text{Ø}12$ BFRP) (a); specimen for compression test wrapped with two layers of ceramic wool (b); black–white pattern at the specimen's surface (c).

The steel plates ($30 \times 30 \times 2$ mm for $\text{Ø}10$ and $50 \times 50 \times 5$ mm for $\text{Ø}8$ and $\text{Ø}12$) were welded with the round pipe pieces ($\text{Ø}20.0 \times 10 \times 2$ mm for $\text{Ø}10$ and $\text{Ø}26.9 \times 12 \times 2$ mm for $\text{Ø}8$ and $\text{Ø}12$). After preparation of the steel caps, they were attached at the ends of FRP bars with the use of epoxy resin and positioned with the use of a spirit level. The length of the bars was 4 cm. In the case of $\text{Ø}12$ bars, the method of specimens' preparation was improved in order to enable examination at higher temperatures. Therefore, cementitious expansive mortar was used instead of epoxy resin.

In the case of specimens tested at elevated temperatures, two layers of ceramic wool (see Figure 2b) were used to sustain the temperature after removing the specimens from the thermal chamber and placing them at the test stand.

In the case of specimens tested at room temperature in both compression and tension, a black–white pattern was added at the surface of the specimens (Figure 2c), so that Digital Image Correlation could be used to determine the strains during the tests, and as a result, moduli of elasticity (at compression and tension) could be calculated.

3. Methods

3.1. Glass Transition Temperature

Glass transition temperature was measured with the use of Discovery DMA 850 (TA Instruments) appliance in Oscillation Temperature Ramp. The specimen was submitted to simultaneous cyclic flexure with the amplitude of deflection equal to 0.8 μm and frequency of 1.0 Hz, and an increase in heating temperature up to 157 $^{\circ}\text{C}$. The heating rate was equal to 2 $^{\circ}\text{C}/\text{min}$.

The storage and loss moduli can be determined using following equations, representing the behaviour of viscoelastic material:

$$\sigma = \sigma_0 \sin(2\pi ft) \quad (1)$$

$$\varepsilon = \varepsilon_0 \sin(2\pi ft - \delta) \quad (2)$$

$$\tan \delta = E'' / E' \quad (3)$$

where:

ε —strain;

ε_0 —strain's amplitude;

σ —stress;

σ_0 —stress's amplitude;

f —frequency;

t —time;

δ —phase lag between stress and strain;

E' —storage modulus;

E'' —loss modulus.

3.2. Tensile Strength and Elasticity at Room Temperature

Average pace of tensile loading was equal to 6 MPa/s. Digital cameras had simultaneously been taking photos from one or two perpendicular directions in set up periods of time.

After the test, photos were analysed in DIC software and, for each specimen, three virtual tensiometers with the length of approximately 100 mm were set on each specimen to calculate strains. Elasticity moduli were calculated as the directional coefficients in linear approximation of stress–strain relations.

3.3. Compressive Strength and Elasticity at Room Temperature

Average pace of compressive loading was equal to 4 Mpa/s. The photos of the specimens were taken during the tests from one or two perpendicular directions in order to determine the strains with the use of DIC software after the tests. The virtual tensiometers with the length of approximately 10 mm were used.

The stress–strain relations for each specimen in compression were calibrated with the use of linear function, where modulus elasticity at compression was assumed as a directional coefficient of these functions. If two digital cameras were used, moduli of elasticity values were calculated on each direction separately.

Compressive strength was calculated as the force at failure divided by the cross-section area.

3.4. Compressive Strength at Elevated Temperatures

Specimens described in Section 2 were heated up till the predetermined value of temperature (up to 100 or 200 °C) was achieved at the surface of the bar. Temperature values were registered with the use of thermocouples mounted under the ceramic wool (see Figure 2b). After removing the specimens from heating chamber, compression tests were performed with the pace of 1.5 mm/min. Maximum forces and temperatures at the surfaces at failure time were registered for each specimen.

4. Results

Results from DMA tests were shown as storage and loss moduli changes (Figure 3). The glass transition temperature determined from loss modulus changes along the temperature growth was equal to 107.5 °C (Figure 3).

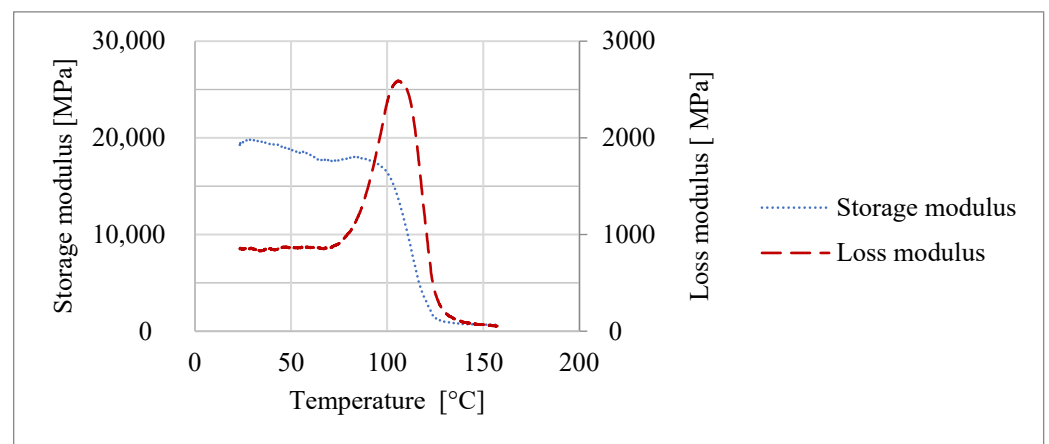


Figure 3. Results from DMA test.

The results from tensile strength tests were summarized (Table 1). The medium values of elasticity modulus were in the range from 43.3 to 44.6 GPa, while tensile strength medium values were 930.5 to 1073.1 MPa.

Table 1. Summary of the results—BFRP bars in tension.

Diameter	Parameter	Specimen No.			Mean Value
		1	2	3	
Ø10 (mounted with epoxy resin)	Tensile strength [MPa]	1143.3	977.8	1098.1	1073.1
	Modulus of elasticity [GPa]	45.6	41.3	47.0	44.6
Ø12 (mounted with epoxy resin)	Tensile strength [MPa]	1121.3	-	-	1121.3 ¹
	Modulus of elasticity [GPa]	44.1	44.1	46.1	44.8
Ø12 (mounted with expansive mortar)	Tensile strength [MPa]	908.4	946.2	936.8	930.5
	Modulus of elasticity [GPa]	45.2, 44.4	43.4, 43.7	42.0, 40.9	43.3 ²

¹ determined only for one specimen. ² mean value calculated on specimens tested from two directions.

Two out of the three Ø12 specimens with caps mounted with epoxy resin did not fail during the test as a result of achieving stresses equal to tensile strength, but the FRP bars with hardened epoxy resin started to slide out of the steel caps. Therefore, maximum strength values should not be considered as tensile strength in that case, and were excluded

from the analysis. Nevertheless, elasticity moduli were calculated for these specimens. Figure 4 shows the typical mode of failure for the analysed specimens.



Figure 4. Specimen after failure in tension.

The results of the compressive tests at room temperature are summarized in Table 2, while Figure 5 shows the typical form of failure in compression. The medium values of compressive strength were in the range of 441.2 to 456.0 MPa, and medium values of elasticity modulus were in the range of 31.0 to 38.4 MPa.

Table 2. Summary of the results—BFRP bars in compression.

Diameter	Parameter	Specimen No.			Mean Value
		1	2	3	
Ø8	Compressive strength [MPa]	416.3	495.8	-	456.0
	Modulus of elasticity [GPa]	27.5, 35.4	35.8, 54.9	-	38.4 ¹
Ø10	Compressive strength [MPa]	434.7	517.5	448.3	466.8
	Modulus of elasticity [GPa]	34.6	28.2	30.2	31.0
Ø12	Compressive strength [MPa]	396.9	521.6	405.0	441.2
	Modulus of elasticity [GPa]	46.9, 50.0	24.5, 24.6	32.8, 37.0	35.1 ¹

¹ mean value calculated on specimens tested from two directions.

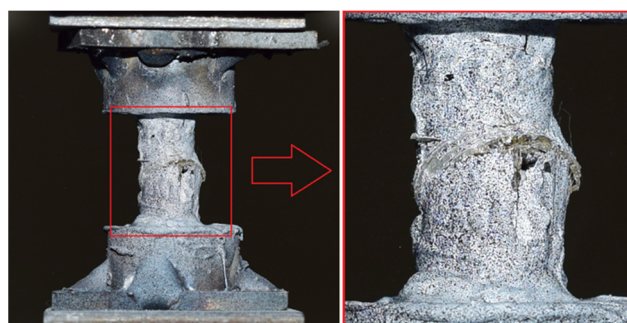


Figure 5. Specimen after failure in compression.

Compressive strength along with temperature at the surface of the specimen at failure time, at compressive strength tests at elevated temperatures (100 °C and 200 °C), are summarized in Table 3. Additionally, the results for four reference specimens tested without heating on the same day are included in this table. The strength retention ratio calculated for the medium temperature at failure equal to 97.3 °C was 24%, and for 191.0 °C, it was 8%.

Table 3. Compressive strength tests during heating results.

Temperature	Parameter	Specimen No.				Mean Value
		1	2	3	4	
20 °C (reference specimens)	Compressive strength [MPa]	497.7	519.5	528.0	472.2	504.3
100 °C	Compressive strength [MPa]	87.1	153.3	120.2	-	120.2
	Temperature at failure [°C]	97	98	97	-	97.3
200 °C	Compressive strength	43.5	49.2	34.1	-	42.3
	Temperature at failure [c]	183	198	192	-	191.0

5. Discussion

Tensile and compressive strength for BFRP bars may strongly vary depending on the type of used matrix, fibres, and volumetric proportions between matrix and fibres.

Basing on a comparison of the results from available experimental studies on mechanical properties of the BFRP bars ([2,3,12–16]—Table 4) the differences between tensile strength may vary from under 600 to even over 1500 MPa, which is a very wide range. In most cases, the tensile strength of the BFRP bars was higher than the typical value of tensile strength for steel reinforcement (about 500–600 MPa). However, no yielding occurs for non-metallic bars. As a result, rupture failure modes were noted in most cases in tension, which may result in a low safe reserve for design purposes.

In terms of tensile strength, the results from this study are similar to the works of Protchenko et al. [13], Urbanski et al. [14] and Włodarczyk and Trofimczuk [16].

Regarding compressive strength of the BFRP bars, there are few data available in the literature concerning this parameter. The reason for that may be the fact that reinforcement bars are typically submitted to tension during their lifecycle in most concrete structures. However, it is worth considering during designing that the compressive strength of the bars can be significantly lower than their tensile strength, and also lower than compressive strength of most of steel reinforcement bars (typically around 500–600 MPa). Moreover, similar results for compressive strength were noted within this study and by Thiyagarajan et al. [3] (about 450–500 MPa).

Elasticity modulus in tension measured within this study was equal to about 45 GPa, which is similar to other studies (38.34–52.0), apart from the Elgabbas et al. studies [2,15], in which the bars had a significantly higher stiffness (59.5–90.4 GPa). Even the highest value of elasticity modulus for BFRP bars amongst the available analysed literature (90.4 GPa) is much lower than typical values for reinforcement steel (about 210 GPa). This may lead to excessive deflections and crack propagation in bent concrete elements with non-metallic reinforcement.

Additionally, this study aimed to experimentally determine elasticity moduli at compression, which were 15–30% lower than the values measured in tension.

Further research will concern the examination of tensile strength at elevated and high temperatures in comparison to the available literature data [17–20]. The results from the current study will also be used for numerical modelling purposes regarding axially compressed concrete columns with BFRP reinforcement bars at room and high temperatures.

Table 4. Mechanical properties of the BFRP bars—comparison.

Reference	Diameters	Tensile Strength [MPa]	Compressive Strength [MPa]	Elasticity Modulus [GPa]
Thiyagarajan et al. [3]	8, 10 and 12 mm	1362.3–1585.6	470.2–495.3	48–52 (tension)
Fan and Zhang [12]	12 mm	569–681	-	-
Protchenko et al. [13]	8 mm	1103.3	-	43.9 (tension)
Urbanski et al. [14]	8 mm	1009.1–1089.4	-	38.34–40.72
Elgabbas et al. [2,15]	7–8 mm	1567–1680	-	59.5–69.0 (tension) 74.0–90.4 (flexion)
Włodarczyk and Trofimczuk [16]	8 and 10 mm	1103–1153	-	43.9–48.2 (tension) 43.3–44.6 (tension)
This study	8, 10 and 12 mm	930.5–1121.3	441.2–466.8	31.0–38.4 (tension) 31.0–38.4 (compression)

6. Conclusions

The following conclusions can be drawn from this study:

1. The mechanical properties of the BFRP may strongly vary depending on many parameters, such as the type of matrix and fibres, and their volumetric proportions. However, there can be noted some trends that are similar to other studies, such as a significant reduction in compressive strength in reference to tensile strength (by over 60% in experiments performed by Thiyagarajan et al. [3] and about 40–50% in this study).
2. Elasticity modulus values determined with the use of Digital Image Correlation for BFRP bars were significantly lower than the values for traditional steel reinforcement (about 5 times lower in tension and 6 times lower in compression).
3. Low glass transition temperature (equal to 107.5 °C), at which structural changes in the material occurred, may lead to significant reduction in possible applicational areas. The same was confirmed in tests at elevated temperatures, as the retention ratio of compressive strength at about 100 °C was equal to 25%, and at 200 °C, it was 8%.

Author Contributions: Conceptualization, M.W. and J.F.; methodology and investigation, M.W., G.S., P.D., N.G. and P.T., writing—original draft preparation, M.W.; visualization, M.W.; supervision, J.F. All authors have read and agreed to the published version of the manuscript.

Funding: This research received no external funding.

Institutional Review Board Statement: Not applicable.

Informed Consent Statement: Not applicable.

Data Availability Statement: Data supporting findings of this study is contained within this article.

Acknowledgments: The publication cost of this paper was covered with funds provided by the Polish National Agency for Academic Exchange (NAWA): “MATBUD’2023—Developing international scientific cooperation in the field of building materials engineering” BPI/WTP/2021/1/00002, MATBUD’2023.

Conflicts of Interest: The authors declare no conflict of interest. The funders had no role in the design of the study; in the collection, analyses, or interpretation of data; in the writing of the manuscript; or in the decision to publish the results.

References

1. Burgoyne, C.; Byars, E.; Guadagnini, M.; Manfredi, G.; Neocleous, K.; Pilakoutas, K.; Taerwe, L.; Taranu, N.; Tepfers, R.; Weber, A. *Technical Report: FRP (Fibre Reinforced Polymer) Reinforcement in RC Structures*; Fédération Internationale du Béton (fib): Lausanne, Switzerland, 2007.
2. Elgabbas, B.; Ahmed, F.; Benmokrane, E. Basalt FRP reinforcing bars for concrete structures. In Proceedings of the 4th Asia-Pacific Conference on FRP in Structures, APFIS, Melbourne, Australia, 11–13 December 2013; Volume 440, pp. 11–13.
3. Thiyagarajan, P.; Pavalan, V.; Sivagamasundari, R. Mechanical characterization of basalt fibre reinforced polymer bars for reinforced concrete structures. *Int. J. Appl. Eng. Res.* **2018**, *13*, 5858–5862.
4. Bank, L.C. *Composites for Construction: Structural Design with FRP Materials*; John Wiley & Sons, Inc.: Hoboken, NJ, USA, 2006.
5. Pareek, K.; Saha, P. Basalt fiber and its composites: An overview. In Proceedings of the National Conference on Advances in Structural Technologies (CoAST-2019), Silchar, India, 1–3 February 2019.
6. Naser, M.Z.; Hawileh, R.A.; Abdalla, J.A. Fiber-reinforced polymer composites in strengthening reinforced concrete structures: A critical review. *Eng. Struct.* **2019**, *198*, 109542. [[CrossRef](#)]
7. Lau, D.; Qiu, Q.; Zhou, A.; Chow, C.L. Long term performance and fire safety aspect of FRP composites used in building structures. *Constr. Build. Mater.* **2016**, *126*, 573–585. [[CrossRef](#)]
8. Siddika, A.; Al Mamun, M.A.; Ferdous, W.; Alyousef, R. Performances, challenges and opportunities in strengthening reinforced concrete structures by using FRPs—A state-of-the-art review. *Eng. Fail. Anal.* **2020**, *111*, 104480. [[CrossRef](#)]
9. Fiore, V.; Scalici, T.; Di Bella, G.; Valenza, A. A review on basalt fibre and its composites. *Compos. Part B Eng.* **2015**, *74*, 74–94. [[CrossRef](#)]
10. Inman, M.; Thorhallsson, E.R.; Azrague, K. A mechanical and environmental assessment and comparison of Basalt Fibre Reinforced Polymer (BFRP) rebar and steel rebar in concrete beams. *Energy Procedia* **2017**, *111*, 31–40. [[CrossRef](#)]
11. Khorramian, K.; Sadeghian, P. Material Characterization of GFRP Bars in Compression Using a New Test Method. *J. Test. Eval.* **2021**, *49*, 20180873. [[CrossRef](#)]
12. Fan, X.; Zhang, M. Experimental study on flexural behaviour of inorganic polymer concrete beams reinforced with basalt rebar. *Compos. Part B Eng.* **2016**, *93*, 174–183. [[CrossRef](#)]
13. Protchenko, K.; Salha, M.; Urbański, M.; Narloch, P. Compressive Properties of BFRP and HFRP Bars. *IOP Conf. Ser. Mater. Sci. Eng.* **2021**, *1015*, 012091. [[CrossRef](#)]
14. Urbanski, M.; Lapko, A.; Garbacz, A. Investigation on concrete beams reinforced with basalt rebars as an effective alternative of conventional R/C structures. *Procedia Eng.* **2013**, *57*, 1183–1191. [[CrossRef](#)]
15. Elgabbas, F.; Ahmed, E.A.; Benmokrane, B. Physical and mechanical characteristics of new basalt-FRP bars for reinforcing concrete structures. *Constr. Build. Mater.* **2015**, *95*, 623–635. [[CrossRef](#)]
16. Włodarczyk, M.; Trofimczuk, D. *Prediction of Ultimate Capacity of FRP Reinforced Concrete Compression Members*; Innovations in Materials, Design and Structures Book of Abstracts for the 2019 fib International Symposium May 27–29; The Institute of Civil Engineering: Delhi, India, 2019; pp. 1353–1361.
17. Hajiloo, H.; Green, M.F.; Gales, J. Mechanical properties of GFRP reinforcing bars at high temperatures. *Constr. Build. Mater.* **2018**, *162*, 142–154. [[CrossRef](#)]
18. Rosa, I.C.; Firmo, J.P.; Correia, J.R.; Barros, J.A.O. Bond behaviour of sand coated GFRP bars to concrete at elevated temperature—Definition of bond vs. slip relations. *Compos. Part B Eng.* **2019**, *160*, 329–340. [[CrossRef](#)]

19. Ashrafi, H.; Bazli, M.; Najafabadi, E.P.; Vatani Oskouei, A. The effect of mechanical and thermal properties of FRP bars on their tensile performance under elevated temperatures. *Constr. Build. Mater.* **2017**, *157*, 1001–1010. [[CrossRef](#)]
20. Najafabadi, E.P.; Oskouei, A.V.; Khaneghahi, M.H.; Shoaie, P.; Ozbakkaloglu, T. The tensile performance of FRP bars embedded in concrete under elevated temperatures. *Constr. Build. Mater.* **2019**, *211*, 1138–1152. [[CrossRef](#)]

Disclaimer/Publisher's Note: The statements, opinions and data contained in all publications are solely those of the individual author(s) and contributor(s) and not of MDPI and/or the editor(s). MDPI and/or the editor(s) disclaim responsibility for any injury to people or property resulting from any ideas, methods, instructions or products referred to in the content.